MNRAS **000**, 000–000 (0000) Preprint 30 October 2017 Compiled using MNRAS LATEX style file v3.0

We are not the 99 percent: quantifying the atypical satellite distributions in the Local Group

Jaime E. Forero-Romero [1] ⋆, Verónica Arias[1]
[1] *Departamento de Física, Universidad de los Andes, Cra. 1 No. 18A-10 Edificio Ip, CP 111711, Bogotá, Colombia*

30 October 2017

ABSTRACT
In this paper we quantify the joint spatial distribution of the brightest satellites around the Milky Way (MW) and M31, the dominant galaxies in the Local Group (LG). We use the Illustris-1 and ELVIS simulations to quantify the expected deviations from statistically spherical satellite distributions in the Lambda Cold Dark Matter paradigm. We estimate that only 0.05% to 0.25% of the pairs with isolation and dynamical characteristics similar to the LG are expected to have satellite distributions with the same degree of deviation from sphericity. This makes the LG a 3σ outlier, with all the weight lying on the extremly planar MW satellite distribution.

Key words: Galaxies: halos — Galaxies: high-redshift — Galaxies: statistics — Dark Matter — Methods: numerical

1 INTRODUCTION

It has been shown that LG pair separation vector is aligned along the filaments in which they are typically embeded Forero-Romero & González (2015), the LG pairs found in pancake-like DM matter arrangements are aligned with the plane itself. Characterizing the satellite alignments with μ thus provide information about how satellites are distributed with respect to the cosmic web.

In Section we list the sources of the observational and simulated data to be used throughout the paper. Next, in Section we describe the methods we use to quantify and characterize the satellite distributions. In section we present our results. In the discussion section we quantify the correlations between the main plane properties as described by the simulations. We use this results to quantify the degree of atipicality of the LG and estimate the volume that has to probed in simulations in order to find a pair with a satellite distribution as atipical as the LG. Finally, we summarize our conclusions in Section .

1.1 Observational Data

1.2 Data from the ELVIS project

1.3 Data from the Illustris project

We use publicly available data from the Illustris Project (Vogelsberger et al. 2014). This suite of cosmological simulations, performed using the quasi-Lagrangian code AREPO (Springel 2010), followed the coupled evolution of dark matter and gas and includes parametrizations to account for the effects of gas cooling, photoionization, star formation, stellar feedback, black hole and super massive black hole feedback. The simulation volume is a cubic box of 75 $\mathrm{Mpc}\,h^{-1}$ on a side. The cosmological parameters correspond to a ΛCDM cosmology consistent with WMAP-9 measurements (Hinshaw et al. 2013).

We extract halo and galaxy information from the Illustris-1 simulation which has the highest resolution in the current release of the Illustris Project. Illustris-1 has 1820^3 dark matter particles and 1820^3 initial gas volumen elements. This corresponds to a dark matter particle mass of $6.3 \times 10^6 \mathrm{M}_\odot$ and a minimum mass for the baryonic volume element of $8.0 \times 10^7 \mathrm{M}_\odot$. The corresponding spatial resolution is 1.4 kpc for the dark matter gravitational softening and 0.7 kpc for the typical size of the smallest gas cell size.

We buid a sample of Isolated Pairs that resemble the conditions in the LG. To construct this sample we select first all galaxies with an stellar mass in the range $1 \times 10^{10}\mathrm{M}_\odot < M_\star < 1.5 \times 10^{11}\mathrm{M}_\odot$. Then we consider the following criteria for all galaxies in that set.

- For each galaxy A we find its closest galaxy B, if galaxy A is also the closest to halo B, the two are considered as a pair.
- With d_{AB} the distance between the two galaxies and $M_{\star,min}$ the lowest stellar mass in the two galaxies, we discard pairs that have any other galaxy C with stellar mass $M_\star > M_{\star,min}$ closer than $3 \times d_{AB}$ from any of the pair's members.
- The distance d_{AB} is greater than 700 kpc.

⋆ je.forero@uniandes.edu.co

• The relative radial velocity between the two galaxies, including the Hubble flow, is -120 km s^{-1} $< v_{AB,r} <$ 0 km s^{-1}.

We find 27 pairs with these conditions. We then select the pairs where in both halos there are at least 15 detected subhalos, thus discarding pairs with halos with the lowest mass. We end up with a total of 20 pairs that fulfill these criteria, Appendix A shows the physical properties (stellar masses, maximum circular velocities, radial velocities and separation) in those pairs.

Although Illustris-1 has stellar particles, we do not use their properties to select the satelite population because the smallest galaxies are barely resolved in stellar mass at magnitudes of $M_V = 9$. We prefer using the dark matter information as the smallest sub-halos are sampled with at least 35 particles. We chose the satellite samples by ranking the subhalos in decreasing order of its maximum circular velocity and select the first N_p halos in the list. The results presented here correspond to $11 \leq N_p \leq 15$.

2 BUILDING, CHARACTERIZING AND COMPARING SATELLITES SPATIAL DISTRIBUTIONS

2.1 Building Satellite Samples

We compare the joint satellite distributions in the MW and M31 at fixed satellite number, N_s. This means that the magnitude cut corresponding to the faintest satellite included in the sample is different in each case. We make this choice for two reasons. First, to be sure that there is a non-zero number of satellites in the simulations to make the computations. Second, to rule out the influence of satellite numbers in the statistics.

We compute the satellite statistics fo 11 up to 15 satellites. The lowest bound corresponds to the number of classical Milky Way satellites. The upper limit corresponds to the maximum number of satellites that can be resolved in both halos for most of the isolated pairs in Illustris-1. In simulations we rank the subhalos by their maximum circular velocity, in observations we rank the satellites by its M_V magnitude.

We also use two kinds of satellite distributions. The first keeps the positions for the satellites fixed as provided in the observations/simulations; the second randomizes the angular positions of the satellites around the central galaxy while keeping its radial distance fixed. The randomization process is done 1000 times for each galaxy.

2.2 Describing Samples with the Inertia Tensor

We base all our results on the description provided by the inertia tensor defined by the satellites's positions.

$$\overline{\mathbf{I}} = \sum_{k=1}^{N_s} [(\mathbf{r_i} - \mathbf{r_0})^{\mathbf{2}} \cdot \mathbf{1} - (\mathbf{r_i} - \mathbf{r_0}) \cdot (\mathbf{r_i} - \mathbf{r_0})^{\mathbf{T}}], \quad (1)$$

where k indexes the set of satellites of interest $\mathbf{r_k}$ are the satellites' positions, $\mathbf{r_0}$ is the location of the central galaxy $\mathbf{1}$ is the unit matrix, and $\mathbf{r}^T$ is the transposed vector $\mathbf{r}$. We use $\mathbf{r_0}$ as the position of the central galaxy, and not the satellites' geometrical center, to allow for a fair comparison once the angular positions of the satellites are randomized around this point.

From this tensor we compute its eigenvalues, $\lambda_1 > \lambda_2 > \lambda_3$, and corresponding eigenvectors, $\hat{I}_1$, $\hat{I}_2$, $\hat{I}_3$. We define the size of the three ellipsoidal axis as $a = \sqrt{\lambda_1}$, $b = \sqrt{\lambda_2}$ and $c = \sqrt{\lambda_3}$. We also define $\hat{n} \equiv \hat{I}_1$ as the vector perpendicular to the planar satellite distribution. We also define the width, w, of the planar satellite distribution, σ_p as the standard deviation of all satellite distances to the plane defined by the vector $\hat{n}$. Finally, we characterize the alignment between the satellite plane and the vector connecting the two dominant galaxies by $\mu = |\hat{r}_{AB} \cdot \hat{n}|$.

To summarize we characterize the satellite distribution by for quantities obtained from the inertia tensor:

- Plane width, w.
- c/a axis ratio.
- b/a axis ratio.
- μ as a measure of plane alignment.

2.3 Comparing Satellite Samples

2.4 Describing joint satellite distributions

3 RESULTS

3.1 Plane Width

Figure 1 summarizes the results for the plane width distributions. The panel on the left compares the results for the MW and M31 observations against its randomized version. The most interesting outcome is that the MW plane width is smaller than 95% of the planes computed from the randomized distribution, while the M31 plane width is consistent with the same distribution.

3.2 c/a axis ratio

3.3 b/a axis ratio

3.4 Plane alignment

Figure 4 summarizes the Illustris results for the alignments between the vector normal to the plane and the vector connecting the two dominant galaxies. The corresponding results for the ELVIS data are shown in Figure B1.

The first striking impression from the left panel in Figure 4 is that the observations are cornered in a region of strong alignment, $\mu \approx 1$, for both galaxies. In other words, the planes are almost perpendicular to the direction connecting the two galaxies. The result for the spherical randomization corresponds to a uniform distribution $0 \leq \mu \leq 1$ as shown in the same panel.

The middle panel tells a similar story for the results from Illustris. That is, there isn't a prefered alignment direction from the simulation. This also holds for ELVIS data. We quantify this visual impresion by performing a K-S test where the null hypothesis corresponds to an uniform distribution. The results from the K-S test do not allow us to discard the null hypotesis.

This information allows us to properly understand the results on the right panel in Figure 4. That panel shows

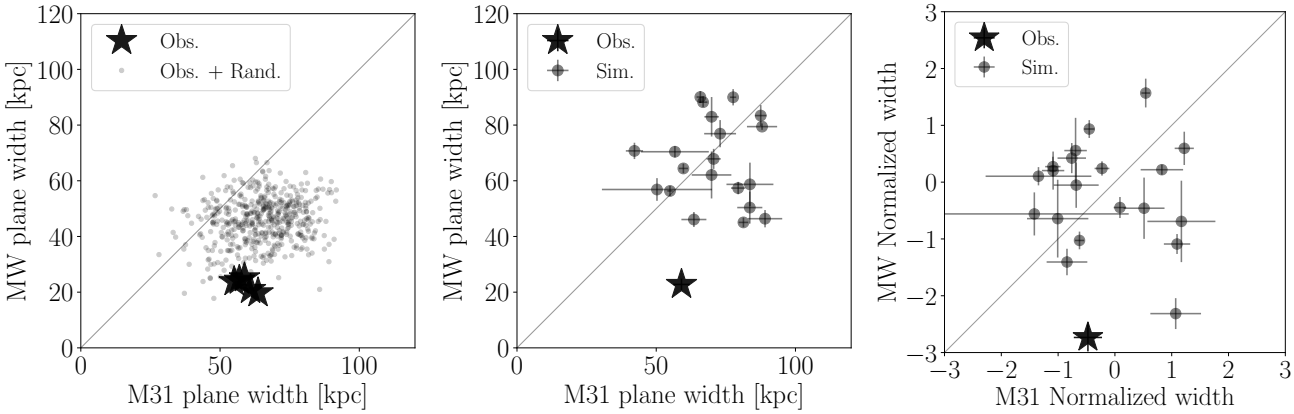

Figure 1. Plane width characterization in the Local Group and the Isolated Pairs. In all panels the horizontal axis corresponds to the M31 or the most massive halo in the pair and the vertical axis to the MW or the least massive halo in the pair. The panel on the left shows the plane width in physical units comparing the results from observations (stars) against the result of spherically randomizing the satellite positions while keeping its radial distance (circles). The panel in the middle compares the average from the observations (star) and the average from each one of the Isolated Pairs (circles with error bars). The panel on the right has the same information as the middle panel, only that this time each point has been normalized (median substracted and normalized by the standar deviation) to the results of its randomization. The main message of this series of plots is that the MW has a significantly thiner plane both compared to the result of its own satellite spherical randomization (left panel) and the expectation from simulations (middle panel). This low value is 2σ away from what is expected in a spherical distribution. In the M31 their satellites are in agreement with the expectations both from an spherical distribution and the results form the simulations. A second conclusion is that the spherically averaged plane width MW (seen in the point cloud in the left panel) is smaller than the average expectation from simulations, while for M31 the spherical average is consistent with simulations.

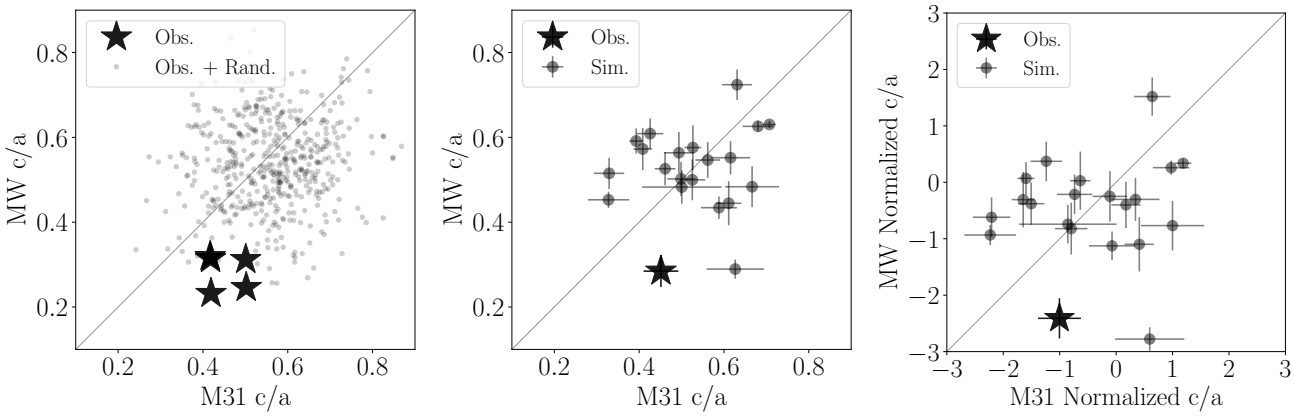

Figure 2. Same layout as in Figure 1. This time for the c/a axis ratio. The message holds in this case as for the plane width. The MW is has a significantly low c/a value compared to the expectation from a spherical distribution and simulations. This low value is also 2σ away from the expactations for an spherical distribution. M31 is consistent both with an spherical distribution and the results from simulations. However, in this case the axis ratio in the spherically averaged case is completeley consistent with the expectation from simulations.

the results for the normalized values to the mean and standard deviation computed from spherically randomized ditributions. In this case the LG μ value has the same probability as any other value (because it is consistent with an uniform distribution) and the apparent large distance from the Illustris data must not be interpreted as an the LG having an atypical alignment.

We defer to the Section **??** our discussion on how this can be reconciled with other studies that show preferential infall satellite directions in LCDM simulations.

4 DISCUSSION

4.1 Outlier characterization with a Multivariate Gaussian Model

Prospects for observational measurement: DESI.

REFERENCES

Forero-Romero J. E., González R., 2015, ApJ, 799, 45
Hinshaw G., et al., 2013, ApJS, 208, 19
Springel V., 2010, MNRAS, 401, 791
Vogelsberger M., et al., 2014, MNRAS, 444, 1518

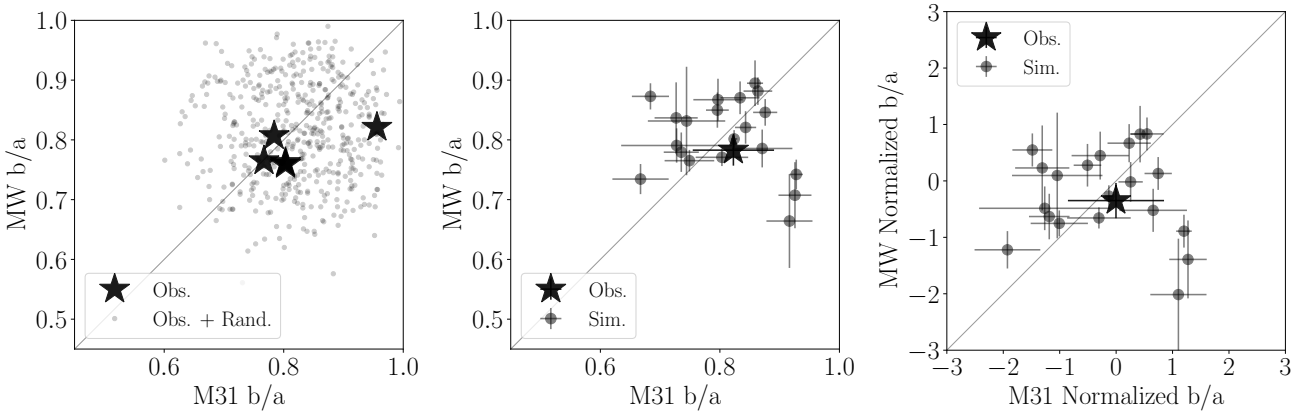

Figure 3. Same layout as in Figure 1. This time for the b/a axis ratio. In this case both the MW and M31 are consistent with the results of a spherical distribution and the simulations.

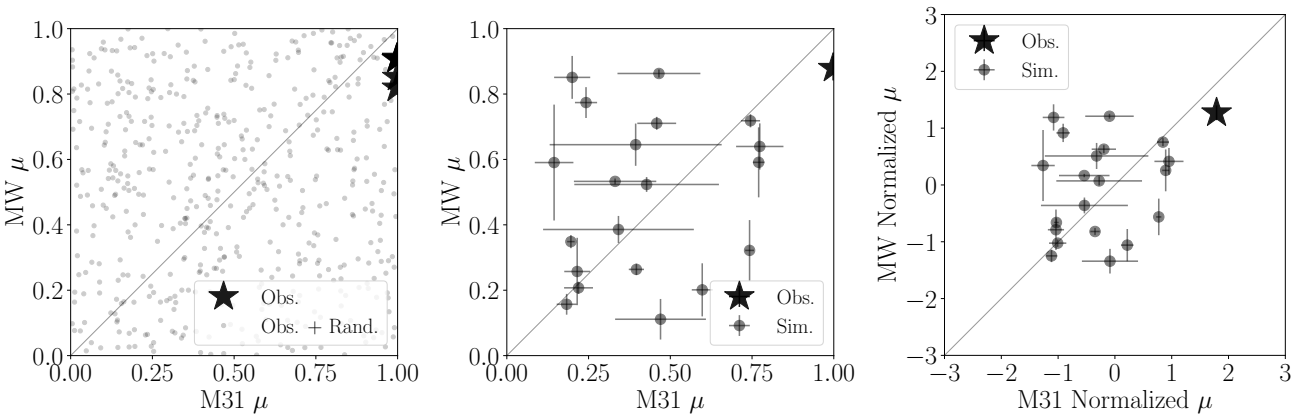

Figure 4. Same layout as in Figure 1. This time for μ the absolute value of the dot product between the vector connecting the main galaxies and the vector perpendicular to the satellite plane. In this case both the MW and M31 show a strong alignment. Apparently the LG is outside the expectations from simulations and atypical compared to the spherical results. However, this is not the case. The μ distributions in the randomization and the simulation are consistent with a uniform distribution. Under such circumstances $\mu \approx 1$ is as likely as any other value.

	Observations		**Randomized Obs.**		**Illustris-1**		**ELVIS**	
	M31	**MW**	**M31**	**MW**	**M31**	**MW**	**M31**	**MW**
Plane width (kpc)	59 ± 3	22 ± 2	64 ± 12	45 ± 8	70 ± 4	67 ± 2	70 ± 2	68 ± 4
c/a ratio	0.45 ± 0.04	0.28 ± 0.03	0.55 ± 0.10	0.53 ± 0.10	0.52 ± 0.01	0.53 ± 0.01	0.54 ± 0.01	0.49 ± 0.02
b/a ratio	0.82 ± 0.06	0.78 ± 0.02	0.82 ± 0.07	0.81 ± 0.08	0.80 ± 0.01	0.80 ± 0.02	0.80 ± 0.01	0.81 ± 0.01

Table 1. Mode Transition Times

APPENDIX A: PHYSICAL CHARACTERISTICS OF THE ISOLATED PAIRS SAMPLES

APPENDIX B: RESULTS FROM ELVIS

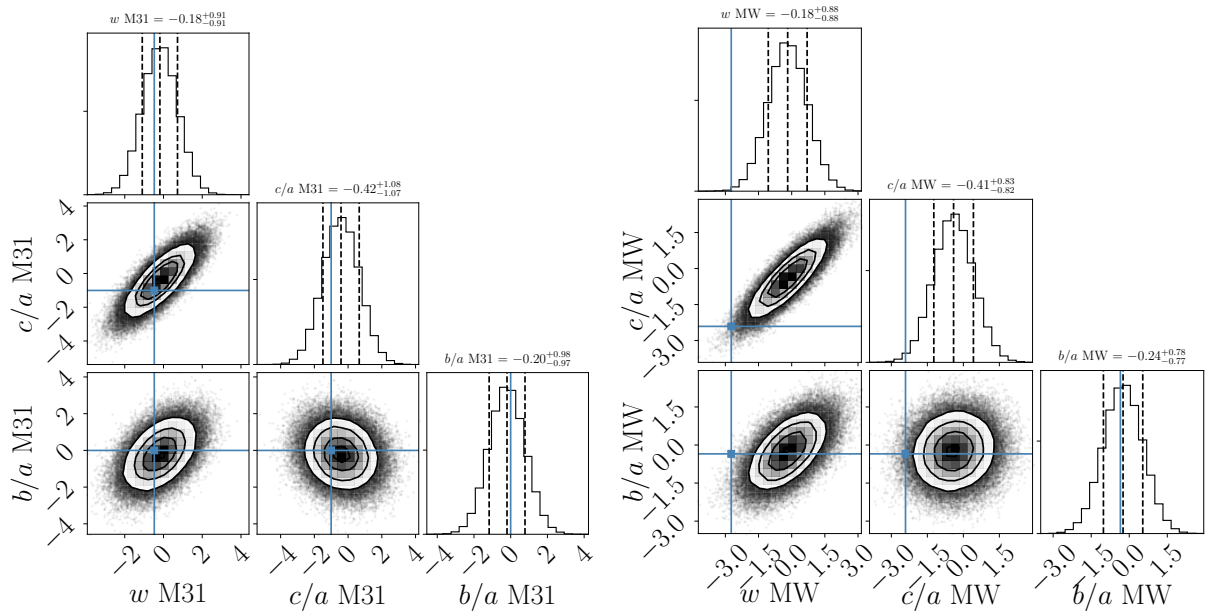

Figure 5. Correlations between the multivariate gaussian model built on the normalized values for the plane width w, c/a ratio and b/a ratio. Left/right panel correspond to M31/MW. The contour levels in the 2D histograms correspond to the 1σ, 2σ and 3σ contours in two dimensions. The dahsed vertical lines in the histograms along the diagonal correspond to the 1σ boundaries in one dimension. The results for the gaussian model are built from 10^6 point realizations in the six-dimensional space spaned by the variables of interest. The correlation matrix and the mean values are computed from the results in the Illustris-1 simulation. The cross indicates the LG values. This plot clearly shows how the M31 results are well within the expectations from simulations while MW has an unusual low value for the plane width and the c/a axis ratio. Equivalent results from the ELVIS data are presented in Figure B2.

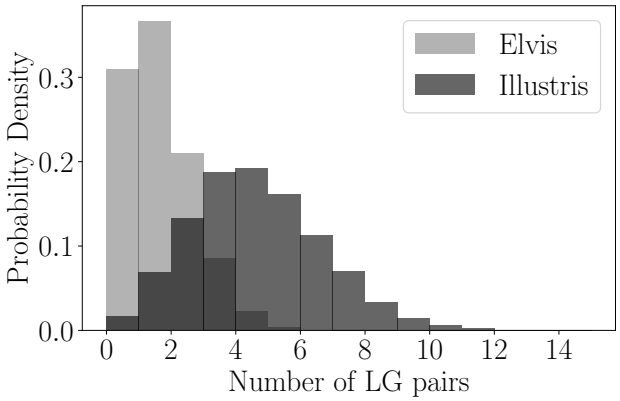

Figure 6. Probability distribution for the expected number of pairs showing the same degree of atipicality as the Local Group if drawn from a sample of 2000 isolated pairs. The distributions correspond to results derived from Illustris-1 and ELVIS data. On average between 0.05% and 0.25% of the isolated pairs should present satellite distributions as atypical as the Local Group.

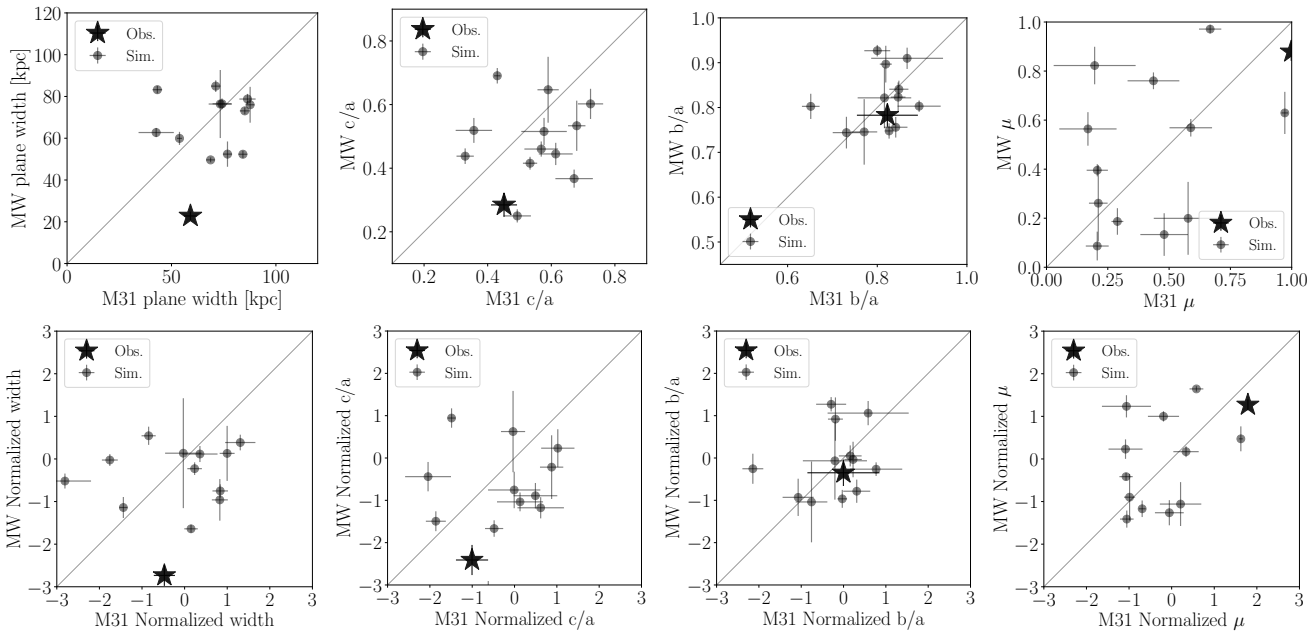

Figure B1. ELVIs results for the quantities presented for the Illustris-1 simulation in Figures 1, 2, 3 and 4. Upper row corresponds to the raw values from observations and simulated pairs, while the second row normalizes the same values to the mean and standard deviation on its spherically randomized counterparts.

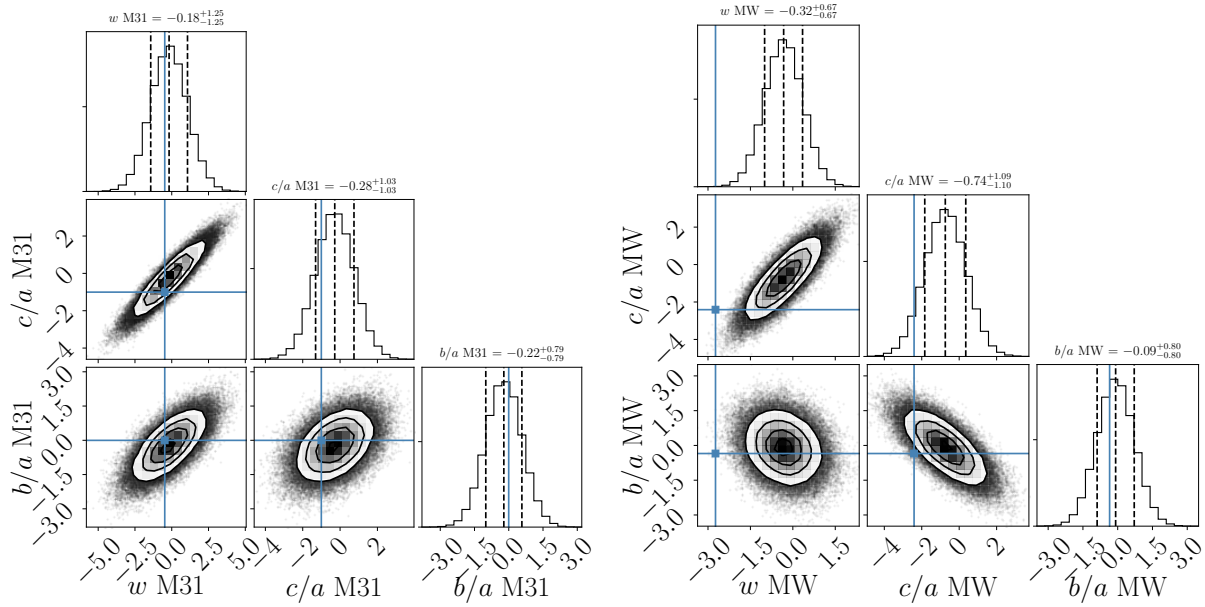

Figure B2. Same layout as Figure 5, this time computed from the ELVIS data.